1-1-2022

Interval Delivery of 5HT2A Agonists Using Multilayered Polymeric Films

Mehjabeen Hossain

INTERVAL DELIVERY OF $5HT_{2A}$ AGONISTS USING MULTILAYERED POLYMERIC FILMS

A thesis
presented in partial fulfillment of requirements
for the degree of Master of Science
in the Department of Biomolecular Sciences
The University of Mississippi

By

MEHJABEEN HOSSAIN

May 2023

ABSTRACT

There is an urgent unmet medical need to develop therapeutic options for the ~50% of depression patients suffering from treatment-resistant depression, which is difficult to treat with existing psycho- and pharmaco-therapeutic options. Classical psychedelics, such as the $5HT_{2A}$ agonists, have re-emerged as a treatment paradigm for depression. Recent clinical trials highlight the potential effectiveness of $5HT_{2A}$ agonists to improve mood and psychotherapeutic growth in treatment-resistant depression patients, even in those who have failed a median of four previous medications in their lifetime. Moreover, microdosing could be a promising way to achieve long-term alleviation of depression symptoms without a hallucinogenic experience. However, there are a gamut of practical barriers that stymie further investigation of microdosing $5HT_{2A}$ agonists, including: low compliance with the complicated dosing regimen, high risk of diversion of controlled substances, and difficulty and cost administering the long-term treatment regimens in controlled settings. Here, we developed a drug delivery system composed of multilayered cellulose acetate phthalate (CAP)/Pluronic F-127 (P) films for the encapsulation and interval delivery of $5HT_{2A}$ agonists from a fully biodegradable and biocompatible implant. CAPP film composition, thickness, and layering strategies were optimized, and we demonstrated three distinct pulses from the multilayered CAPP films in vitro. Additionally, the pharmacokinetics and biodistribution of the 5HT2A agonist 2,5-Dimethoxy-4-iodoamphetamine (DOI) were quantified following the subcutaneous implantation of DOI-loaded single and multilayered CAPP films. Our results demonstrate, for the first time, the interval delivery of psychedelics from an implantable drug

delivery system and open the door to future studies into the therapeutic potential of psychedelic delivery.

DEDICATION

This thesis is dedicated to people who are suffering from major depressive disorder,

I know how you feel.

LIST OF ABBREVIATIONS AND SYMBOLS

CAP	Cellulose Acetate Phthalate
P	Pluronic F-127
MDD	Major Depressive Disorder
TRD	Treatment-resistant Depression
DOI	2,5-Dimethoxy-4-iodoamphetamine
FSH	Follicle-Stimulating Hormone
LH	Luteinizing Hormone
LHRH	Luteinizing Hormone-Releasing Hormone
PVA	Polyvinyl Alcohol
F-68	Poly(ethylene oxide)-poly(propylene oxide)-poly(ethylene oxide) Triblock Copolymer
PNIPAAM	Poly(N-isopropylacrelamide)
P(AMPS-co-BMA)	Poly(2-acrlamide-2-methylpropanesulfonic acid-co-butyl methacrylate)
EVAc	Ethylene and Vinyl Acetate Matrix
PSA	Poly(sebacic) acid
PBS	Phosphate Buffer Saline
HPLC	High-Performance Liquid Chromatography
PLGA	Poly(lactic-co-glycolic acid)
LSD	Lysergic Acid Diethylamide
SEM	Scanning Electron Microscopy

ACKNOWLEDGMENTS

First and foremost, I would like to express my sincere gratitude to my research advisor Dr. Thomas A. Werfel, for his support, and guidance throughout the program. I would like to thank my committee members, Professor Willett, Dr. Smith, Dr. Ashpole, and Dr. Paris, for their insightful comments and suggestions. I want to express my gratitude to all the faculty members, staff, and students of the department of BioMolecular Sciences. I would like to thank all the Interdisciplinary Nanobiosciences lab members with whom I worked.

Gratitude to my husband Md Imdadul H. Khan and my daughter Ilayna Khan. Last but not least, almighty Allah. Thank you for all the blessings I have not even asked for! May we find purpose in where our passion lies.

TABLE OF CONTENTS

Abstract	iii
Dedication	iv
List of Abbreviations and Symbols	v
Acknowledgments	vii
List of Figures	ix
List of Tables	xi
1. Introduction.	1
1.1. Pulsatile Drug Delivery.	1
1.2. Types of Pulsatile Drug Delivery Systems.	2
1.2.1 Time-controlled Pulsatile Delivery System.	2
1.2.2. Stimuli-responsive Delivery System.	3
1.2.3. Externally-controlled Pulsatile Delivery System.	4
1.3. Disadvantages of Current Pulsatile Delivery Devices.	5
1.4. Major Depressive Disorder and Current Challenges in Therapy.	6
1.5. Our Approach for 5HT2A agonist delivery.	8
2. Materials and Methods	10
2.1. Materials.	10
2.2. Fabrication of CAPP Films.	10

2.3. Fabrication of Multilayered CAPP Films.	10
2.4. Measuring Drug Release Kinetics from Single and Multilayered CAPP Films.	11
2.5. PBS Absorption Study.	11
2.6. Visualization of CAPP Film Layers.	11
2.7. Animals.	12
2.8. Pharmacokinetic Assay.	12
2.9. UPLC-MS/MS Identification and Quantitation of DOI.	13
2.10. Statistics.	13
3. Results	15
3.1. Preparation of CAPP Polymer Films.	15
3.2. Optimization of the CAPP "Release" Layer.	17
3.3. Release of the 5HT2A Agonist DOI from CAPP Films.	19
3.4. Optimization of the CAPP "Blank" Layer.	20
3.5. Interval Release of Multilayered CAPP Films.	23
3.6. In Vivo Interval Delivery of DOI from Multilayered CAPP Films.	24
4. Discussion	27
5. Conclusion & Future Direction	32
References	34
Appendix	38
Vita	46

LIST OF FIGURES

Figure 1. Schematic of CAPP film preparation. (A) Schematic of CAPP film formation by solvent evaporation and drug encapsulation. (B) Representative images of the film production process.	15
Figure 2. Optimization of the CAPP "release" layer. (A) Film thickness vs. polymer mass. (B) SEM images of cross-sections 0.1-, 0.2-, 0.3-, 0.4 mm films (clockwise) (C) Erosion time vs. film thickness. (D) Cumulative release of Rhodamine from 0.1-0.4 mm films.	17
Figure 3. DOI release from single-layered CAPP film *in vitro* and *in vivo*. (A) *In vitro* cumulative release of DOI from 0.1 mm CAPP films. (B) Scheme of subcutaneous implantation and experimental time course. (C-F) Pharmacokinetics and biodistribution of DOI released from subcutaneously implanted, single-layered CAPP films in vivo. (n = 4)	19
Figure 4. Optimization of the CAPP "Blank" Layer. (A) Water absorption for 70:30-90:10 CAPP films measured by mass of the films before and after incubation in PBS. B) Erosion time for 70:30-90:10 CAPP films at each thickness 0.1-0.4 mm. (C-F) Rhodamine release from 70:30 vs 90:10 films at each thickness 0.1-0.4 mm. (n = 3)	22
Figure 5. Characterization of Multilayer CAPP films. (A) Schematic representation of multilayer CAPP film design. (B) Representative confocal microscopy image of a multilayered CAPP film cross-section. *Differences in shading are present because it	23

was not possible to get the entire films in a single focal plane. (C) Rhodamine release from Multilayer CAPP films with 3 total doses as indicated in part (A). (n = 3)	
Figure 6. *In vivo* delivery of DOI from multilayer CAPP films. (A-D) Concentration of DOI in plasma (A), brain (B), liver (C), and kidneys (D) from 2-28 hours post-implantation of multilayered CAPP films. (n = 4)	25

LIST OF TABLES

Table 1: Erosion Time vs. Film Thickness	39
Table 2: Cumulative release of Rhodamine from 0.1-0.4 mm films.	39
Table 3: *In vitro* cumulative release of DOI from 0.1 mm CAPP films.	40
Table 4: Concentration of DOI in mouse plasma at different time points after implantation of a single DOI-loaded 0.1 mm film	40
Table 5: Concentration of DOI in mouse brain at different time points after implantation of single DOI-loaded 0.1 mm film	41
Table 6: Concentration of DOI in mouse liver at different time points after implantation of a single DOI-loaded 0.1 mm film	41
Table 7: Concentration of DOI in mouse kidney at different time points after implantation of a single DOI-loaded 0.1 mm film	42
Table 8: Water absorption for 70:30-90:10 CAPP films measured by mass of the films before and after incubation in PBS	42
Table 9: Erosion time for 70:30-90:10 CAPP films at each thickness 0.1-0.4 mm	43
Table 10: Concentration of DOI in mouse plasma at different time points after implantation of multilayered DOI-loaded film	43

Table 11: Concentration of DOI in mouse brain at different time points after implantation of multilayered DOI-loaded film	44
Table 12: Concentration of DOI in mouse liver at different time points after implantation of multilayered DOI-loaded film	45
Table 13: Concentration of DOI in mouse Kidney at different time points after implantation of multilayered DOI-loaded film	45

Thank you for your order!

Dear Mehjabeen Hossain,

Thank you for placing your order through Copyright Clearance Center's RightsLink® service.

Order Summary

Licensee:	University of Mississippi
Order Date:	Mar 19, 2023
Order Number:	5512510663854
Publication:	JOURNAL OF BIOMEDICAL MATERIALS RESEARCH PART A
Title:	Interval delivery of 5HT2A agonists using multilayered polymer films
Type of Use:	Dissertation/Thesis
Order Total:	0.00 USD

View or print complete details of your order and the publisher's terms and conditions.

Sincerely,

Copyright Clearance Center

customercare@copyright.com
https://myaccount.copyright.com

CHAPTER 1

INTRODUCTION

1.1. Pulsatile Drug Delivery

Pulsatile drug delivery is the rapid release of a given amount of drug following a predefined off-released period [1]. Traditional drug delivery systems (oral, subcutaneous, intravenous, etc.) deliver the complete dose immediately after administration in order to achieve quick systemic drug absorption. This can cause the plasma drug concentration to instantly rise and then fall to a subtherapeutic level, in many cases requiring multiple oral, intravenous, or subcutaneous administrations in a relatively short time period to effectively treat the disease [2]. In some other types of delivery systems, a sustained therapeutic effect is ensured by keeping the drug concentration in the therapeutic window for an extended period of time. Such a release pattern may not be appropriate in certain circumstances, which require the release of the drug after a certain lag period [3]. In other words, they need a pulsatile drug delivery system. The treatment of disorders such as hypertension, rheumatoid arthritis, myocardial infarction, etc. exhibits circadian rhythms in their pathophysiology requiring pulsatile drug delivery [4]. Numerous other circumstances necessitate pulsatile release, including many circadian-rhythmic physiologic processes, such as the secretion of hormones (follicle-stimulating hormone (FSH), luteinizing hormone (LH), luteinizing hormone-releasing hormone (LHRH), estrogen, and progesterone), stomach acid secretion, gastric emptying, and gastrointestinal blood transfusion [3]. The development of a pulsatile delivery platform can also help with ease of access to therapy, and compliance with the complex therapy regimen.

1.2. Types of Pulsatile Drug Delivery Systems

Pulsatile drug delivery system or on-delivery drug delivery system can be divided broadly into three categories based on drug release mechanisms. i) Time-controlled pulsatile delivery system ii) Stimuli-responsive pulsatile delivery system iii) Externally-controlled pulsatile delivery system [3].

1.2.1 Time-Controlled Pulsatile Delivery System

Bulk erosion refers to a situation where water enters a polymer more quickly than the polymer degrades. This leads to a gradual degradation process that occurs throughout the polymer sample until a critical molecular weight is reached. At this point, the degradation products become small enough to dissolve, which results in the polymer structure becoming more porous and hydrated. Consequently, the release of the drug from the polymer is delayed until the critical molecular weight is reached. Researchers have explored the use of this system for potential formulations [5].

Surface erosion is another type of polymer degradation that occurs only on the surface and is proportional to the surface area. This process is heterogeneous, meaning that the degradation rate varies depending on the polymer. In surface-eroding systems, drug release is often predictable and correlated with the erosion rate, which is desirable for many drug delivery applications. The erosion process starts from the outside and progresses towards the interior of the polymer. In general, thicker systems take longer to erode, while hydrophilic polymers degrade faster than hydrophobic ones [6].

The release of drug can also be regulated by incorporating a rupturable outside coating layer. The coating can be ruptured by various means, including the use of effervescent excipients, swelling agents, or osmotic pressure, which generate the necessary force to break the coating and

release the drug. As the thickness and hardness of the core tablet increases, so does the amount of time it takes for the drug to be released. This delay is known as the "lag time" [7].

Another interesting invention using time-controlled release is Pulsincap (Michigan) [3]. It is an enteric polymer-coated capsule-shaped device, which has two parts. The non-disintegrating part containing the drug is sealed with a hydrogel plug in the opening. The hydrogel plug itself is covered by a water-soluble coating. As a result, when the capsule comes in contact with fluid, the hydrogel plug swells, and after a lag period, it pushes out the drug in the stomach. A modification of this device was in a form of a granule or bead. In the bead, the same principle applies to four spherical layers including a core, a drug, a swelling agent (e.g., sodium starch glycolate or carboxy methyl cellulose sodium), and an outer membrane of water-insoluble polymer (e.g., ethyl cellulose, Eudragit® RL). Another version of the Pulsincap was made by Patel and Patel, who used diclofenac sodium in order to target the colon [3].

1.2.2 Stimuli-Responsive Delivery System

There has been a plethora of on-demand delivery system which use stimuli responsiveness. The stimuli can be temperature, ultrasound, magnetic field etc. Hydrogels are frequently used in thermosensitive delivery. Hydrogels are a crosslinked biologic, synthetic or semi-synthetic polymers. A type of hydrogel can form in situ gels in lower temperature (close to room temperature) and undergo volume shrinkage in higher temperature when put in body [3].

For example, Sang Oh et al. created drug delivery systems that are sensitive to temperature using a mixture of poly(ethylene oxide)-poly(propylene oxide)-poly(ethylene oxide) triblock copolymer (F-68) and polyvinyl alcohol (PVA) [8]. These systems were designed to release acetaminophen in a pulsatile manner in response to changes in temperature, specifically between 35 °C and 40 °C.

The development of a chemical-responsive drug delivery system has been a much-researched topic in this field. The chemicals can be anything [3], such as, the presence of a specific molecule, a change in pH, the presence of a specific enzyme, or the presence of reactive oxygen species. An innovation in this field was the production of polymeric gels made of PNIPAAM with phenylboronic acid moieties which undergo volume change in presence of glucose. This type of drug delivery system can be desirable to deliver on-demand insulin in the patient when there is high blood glucose present, as the high glucose work as the chemical signal which ensures the release of drug from the polymer [9].

Other stimuli that has been used in many aspects is radiotherapy stimulation to deliver drug. Radiotherapy has been used to effectively deliver Doxorubicin, a chemotherapeutic drug. Gold nanoparticles (Au-NP) have been used as radiosensitizers. A Pluronic F-127 gel loaded with Au and Dox was made (Au-Dox-gel) and showed sustained release of Au and Dox under radiotherapy stimulation [10].

1.2.3 Externally-Controlled Pulsatile Delivery System

One of the earliest approaches investigated to create an externally controlled drug delivery system was the use of an oscillating magnetic field to regulate the release of drugs from a polymer matrix. Magnetic carriers containing materials like magnetite, iron, nickel, and cobalt respond to a magnetic field, making them useful in this type of system. To be suitable for biomedical applications, magnetic carriers must be biocompatible, non-toxic, non-immunogenic, and water-soluble. The speed of drug movement through the stomach and intestines can then be controlled by an external magnet, allowing for the timing and extent of drug absorption to be adjusted [11], [12].

Electrically responsive delivery systems are made using polyelectrolytes, which makes them sensitive to changes in both pH and electric fields. When an electric field is applied, the hydrogels used in these systems may swell, de-swell, or erode. One example of an electrically responsive drug delivery system is the one that uses Poly(2-acrlamide-2-methylpropanesulfonic acid-co-butyl methacrylate) P(AMPS-co-BMA) hydrogels, which can be activated by electric stimuli to release drugs [3].

Ultrasound is commonly used to improve drug permeation through various biological barriers, such as skin, lungs, intestinal walls, and blood vessels. It is often used as an enhancer in controlled drug delivery systems, and there are several reports that demonstrate its effectiveness. Scientists were able to achieve a 27-fold increase in the release of 5-fluorouracil from an ethylene and vinyl acetate (EVAc) matrix by using ultrasound. As the strength of the ultrasound increased, so did the amount of 5-fluorouracil release [13].

1.3. Disadvantages of Current Pulsatile Drug Delivery Devices

Pulsatile drug delivery devices are designed to release medication in a controlled, pulsatile manner, mimicking the body's natural release of certain hormones or drugs. However, these devices have some shortcomings.

One issue with certain pulsatile drug delivery devices is that they may be made with non-biodegradable materials, which can require two surgeries for implantation and removal [14]. This is because non-biodegradable materials may cause an inflammatory response or other adverse reactions in the body over time. As a result, they may need to be removed after a certain period, which requires a second surgery**.**

In addition to being invasive, some pulsatile drug delivery devices may require the patient to carry an external device to ensure proper delivery. This can be inconvenient and may affect the

patient's quality of life. Pulsatile release of drugs require multiple administration throughout the week, which can lead to non-compliance.

Some devices require external electrochemical [15] or thermochemical stimuli [16]to trigger drug release. These external stimuli may be difficult to control and not very accessible to everyone.

To address these issues, researchers are working on developing new pulsatile drug delivery devices that are biodegradable, less invasive, and do not require external stimuli.

1.4 Major Depressive Disorder and Current Challenges in Therapy

Depression is a major public health burden domestically and worldwide, costing the USA alone more than $326.2 billion annually (2020 value) [17]. Treatment options for patients with major depressive disorder (MDD), consist primarily of psychotherapy and pharmacotherapy. Primary challenges to the treatment of MDD are the relatively low response rates to medication as well as high relapse in a large subset of patients. The most comprehensive study of MDD undertaken was the National Institute of Mental Health–funded Sequenced Treatment Alternatives to Relieve Depression (STAR*D) trial [17]. The trial outlined an algorithmic, sequential treatment approach and thus allows for an estimated likelihood of antidepressant success with subsequent trials [17]. Acute remission rates declined with each additional trial (trial 1, 37%; trial 2, 31%; trial 3, 14%; trial 4, 13%). Correspondingly, the probabilities of remitting and maintaining remission for 1 year decrease with each additional trial (26% for level 1, 14% for level 2, 5% for level 3, and 3% for level 4). Unfortunately, this corresponds to over 43% of patients who fail the first two trials. Given the steep decline in remission rates and poor prognosis after the first two trials, these patients are classified as having treatment-resistant depression (TRD). On average, patients defined as treatment-resistant have more severe depression; more past suicide attempts; more hospitalizations; longer episodes; receive more benzodiazepines, antipsychotics, and

electroconvulsive therapy; and experience job loss and financial stress more frequently than patients with MDD that is responsive to therapy [18].

Classical psychedelics have re-emerged as a novel treatment paradigm for depression with the potential to address the shortcomings of current therapies in TRD patients. The classical psychedelics span a number of chemical classes, but the most common shared feature is their activity at the serotonin 2A receptor ($5HT_{2A}$) [19]. The first major, modern clinical trial to explore the utility of psychedelics in TRD was published in 2016 by Carhartt-Harris and colleagues [20], with a follow up study in 2018 [21]. In this open-label feasibility trial, 20 patients with moderate-to-severe unipolar TRD received two oral high-doses of psilocybin with psychological support before, during, and after each session. Patients in the study had failed a median of four medications in their lifetime, placing them amongst the most treatment-resistant and poorest prognosis patients when benchmarked against those in the STAR*D study. Applying the conservative response criterion used in this study, nine patients were responders (45%) with six of these nine maintaining response at six months (30%). A model of psychedelic-induced $5HT_{2A}$ receptor signaling causing an acute change in plasticity and increased global integration in the brain was proposed by the authors as a mechanism to these changes [22][23][24].

Although classical psychedelics that agonize $5HT_{2A}$ (e.g., psilocybin) show therapeutic promise for TRD patients, there are a gamut of practical barriers that could limit the widespread acceptance of their use as therapeutic agents. Obvious major hurdles to furthering the research on $5HT_{2A}$ agonists such as lysergic acid diethylamide (LSD), psilocybin, and others are their status as Schedule I drugs and the hallucinogenic response to the drugs at high doses. Current clinical trials for full-dose treatment with $5HT_{2A}$ agonists require the presence of two therapists during the ~6-8-hour session [25]. This human capital-intensive model of treatment is unlikely to scale and

will not be accessible for patients outside of close proximity to a well-resourced research hospital. 'Microdosing', or the ingestion of sub-perceptual doses of psychedelics every 3-7 days, is a potential alternative approach that has gained momentum in the lay public. And recently, the first human clinical trial investigating the effects of four low doses of LSD was published and established dose-response relationships for various behavioral and physiological effects [26]. More research is needed to establish the potential of microdosing to improve the symptoms of TRD, but practical barriers will limit this approach as well. Specifically, patient compliance to the complex treatment regimen involved with microdosing is likely to be very low. Moreover, there will be concerns about the abuse and diversion of psychedelics that prevent patients from taking the drugs at home and necessitate burdensome and costly trips to a clinical site for every microdose. Therefore, the success of this therapeutic modality may rely heavily on the ability to produce drug delivery systems that can overcome the challenges of abuse/diversion, compliance, and accessibility. Moreover, as opposed to traditional long-term controlled release, these drug delivery systems will need to be optimized for intermittent delivery with precisely defined intervals.

1.5. Our approach for $5HT_{2A}$ agonist Delivery

Polymeric films composed of a mixture of Cellulose Acetate Phthalate (CAP) and Pluronic F-127 (P) (i.e., CAPP polymer films) can be produced to encapsulate a broad range of compounds and control drug release by optimizing the film degradation kinetics [27][28][29][30]. To this end, CAP and P polymers are mixed in a volatile solvent (e.g., acetone) and allowed to dry into CAPP films via solvent evaporation. The films are formed through polymer secondary interactions driven by hydrogen bonding between CAP and P as well as physical entanglement of the polymers. Because of the hydrophobicity of CAP, it has been established that films with a high ratio of CAP

(~60% and above) surface erode, whereby degradation proceeds from the exterior surface of the films [27] . Achieving surface erosion is an essential design criterion for the ordered release of microdoses based on the stacking of alternating layers of drug-loaded and unloaded films. Importantly, CAPP films can be used to encapsulate a wide variety of drugs, which are released in a controlled manner upon degradation of the CAPP films in aqueous environments. CAPP films are also highly biocompatible and have been used in previous work for the sequential delivery of drugs to improve bone regeneration and dental health [27][31][32][33]. Here, we optimized multilayered CAPP films to achieve interval delivery of the $5HT_{2A}$ agonist and psychedelic 2,5-Dimethoxy-4-iodoamphetamine (DOI), monitoring drug release in vitro as well as the pharmacokinetics and biodistribution of DOI released from subcutaneous implants *in vivo*.

CHAPTER 2

MATERIALS AND METHODS

2.1. Materials

Cellulose Acetate Phthalate (Millipore Sigma), Pluronic F-127 (Milipore Sigma), Rhodamine B (Fisher Scientific), 2,5-dimethoxy-4-iodoamphetamine (Cayman Chemical), PBS pH 7.4 (Thermofisher Scientific), Acetone (Sigma-Aldrich), Poly(sebacic acid), diacetoxy terminated (Sigma-Aldrich).

2.2. Fabrication of CAPP Films

CAP and P polymers were mixed at a weight ratio of 70:30, 80:20, and 90:10 to obtain final masses of 300, 600, 900, and 1200 mg. The polymer mixtures were then dissolved in acetone at 7% w/v ratio. Rhodamine or $5HT_{2A}$ agonists (1050 μg DOI/rhodamine for ~70, 6 mm diameter films) were added so that each 6 mm film contained 15 μg of active compound. The polymers or polymer/drug mixtures were next poured into Teflon dishes and kept refrigerated at 4 °C for slow evaporation. After 24 hours, dried films were removed from the Teflon dishes and stored at room temperature until usage. Films 6 mm in diameter were excised from the bulk films using single hole puncher utensils, and film thicknesses were measured using digital calipers.

2.3. Fabrication of Multilayered CAPP Films

To produce multilayered CAPP films, drug-loaded films were arranged in the desired sequence with alternating layers of unloaded, “blank” CAPP films. Each layer in the stack of CAPP films was bonded together by the application of 5 μL of acetone, followed by rapid compression and bonding to the subsequent layer. After assembly of all layers, the multilayered CAPP films

were then coated with poly(sebacic acid) (diacetoxy-terminated: PSA, Sigma-Aldrich) on all sides but one to ensure unidirectional erosion of the CAPP films. To coat with PSA, acetone was added to the PSA powder until it produced a paste-like consistency. Subsequently, a spatula was used to directly coat the paste of PSA onto the bottom and sides of the multilayer films.

2.4. Measuring Drug Release Kinetics From Single and Multilayered CAPP Films

For single-layer drug release studies, CAPP films of thicknesses varying from 0.1 – 0.4 mm were submerged in 1.5 mL of phosphate buffer saline (PBS) and incubated at 37 °C. Supernatants were gathered every 8 hours, followed by the measurement of rhodamine fluorescence using a microplate reader (BioTek Synergy H1) at 546/568 nm (excitation/emission) until films were fully dissolved and no more rhodamine signal was observed. For films loaded with the $5HT_{2A}$ agonist DOI, films were submerged in 1.5 mL of PBS at 37 °C and supernatants were gathered every 8 hours. DOI concentrations were quantitated by high-performance liquid chromataography (HPLC) according to the method below.

2.5. PBS Absorption Study

CAPP films 0.4 mm thick and varying in CAP:P ratio (70;30, 80:20, and 90:10) were fabricated and then submerged in equal volumes of PBS. The mass of the CAPP films was measured prior to submersion in 1.5 mL of PBS (0 mins). After 15 mins and 30 mins incubation in PBS, the CAPP films were removed from solution, dried, and their masses were recorded again.

2.6. Visualization of CAPP Film Layers

CAPP films of different thickness (0.1, 0.2, 0.3, and 0.4 mm) were visualized using a JSM-7200 FLV Field-Emission Scanning Electron Microscope (FESEM)[18]. Multilayered CAPP films were produced with the following layering strategy: Layer 1 (0.1 mm, Rhodamine), Layer 2 (0.8 mm, Blank), Layer 3 (0.1 mm, Rhodamine), Layer 4 (0.8 mm, Blank), Layer 5 (0.1 mm,

Rhodamine), Layer 6 (0.8 mm, Blank). Multilayered films were sliced down the middle using a single-edged razor blade. After cutting the multilayered films in half, confocal microscopy was performed to image the cross-section of the multilayered films using a Leica SP8 confocal microscope.

2.7. Animals

Experiments were performed on adult (9-12 weeks old) CD-1 mice (Charles River). All procedures were performed in compliance with the University of Mississippi Institutional Animal Care and Use Committee (IACUC #22-003) and following the National Institutes of Health (NIH) guidelines. Animals were housed in cages with up to 4 littermates at 12 hours light/dark cycle at 23 °C with food and water ab libitum. To account for sex as a biological variable, a 50:50 ratio of M:F mice was used for all studies reported here.

2.8. Pharmacokinetic Assay

Single or multilayered films containing DOI were implanted subcutaneously on the dorsal side of CD-1 mice. Multilayered CAPP films were composed with the following layering strategy: Layer 1 (0.1 mm, DOI), Layer 2 (0.8 mm, Blank), Layer 3 (0.1 mm, DOI), Layer 4 (0.8 mm, Blank), Layer 5 (0.1 mm, DOI), Layer 6 (0.8 mm, Blank), PSA coating on all sides other than the top of Layer 1. As a vehicle control, blank CAPP films were implanted in one cohort of mice. In each group (n=4), mice were euthanized at 2, 4, 8, 12, 16, 20, 24, and 28 hours after implantation. Blood was collected by cardiac puncture and stored in K2 EDTA tubes. Mice were then perfused with PBS, followed by harvest of the heart, lungs, liver, spleen, kidneys, and brain which were frozen on dry ice immediately following excision. Plasma was separated from the cells by centrifugation at 2000 rcf for 20 minutes and collecting the top layer. Tissues and plasma were stored at -80 °C until further analysis.

2.9. UPLC-MS/MS Identification and Quantitation of DOI

A simple protein precipitation method was followed for extraction of DOI from mice plasma. To an aliquot of 50 µL of plasma or tissue (brain, liver or kidney) samples, phenacetin (internal standard, IS) solution (5 µL of 20 ng/mL) was added and mixed for 15 s on a cyclomixer (Thermo Scientific, IN, USA). After precipitation with 200 µL of acetonitrile, the mixture was vortexed for 2 min, followed by centrifugation for 10 min at 14,000 rpm on an accuSpin Micro 17R (Fisher Scientific, USA) at 5 °C. An aliquot of ~150 µL of clear supernatant was transferred into vials and 2 µL was injected onto LC-MS/MS system for analysis.

Chromatography was performed on an AcquityTM UPLC system (Waters Corp, Milford, MA) with an autosampler temperature at 10 °C. Waters Acquity UPLC® HSS C18 column (3.0×50 mm, 1.8 µm particle size) was used for chromatographic separation with linear gradient elution consisting of (A) 90% acetonitrile and (B) 10% 0.2% formic acid in Milli-Q water as mobile phases. The flow rate was set at 0.30 mL/min, and the injection volume was 2 µL.

An Acquity Tandem Quadrupole Mass Detector (Xevo TQ-S; Waters Corp, Milford, MA) in positive electrospray ionization mode was used for mass spectrometric detection. For collision-induced dissociation, argon was used as collision gas. The cone voltage and collision energy were set at 34 V and 30 V for DOI and 46 V and 26 V for the IS, respectively. Quantification was performed using the monitoring of multiple reaction monitoring (MRM) of following transitions: m/z 322/134 for DOI and m/z 180/92.7 for IS. Retention times of DOI and IS were 1.69 and 1.89 minutes, respectively.

2.10. Statistics

Unless indicated otherwise, data are represented as average with a standard error of the mean (SEM). For comparison of the mean of the two groups, Student's T-test was used. analysis

of variance (ANOVA) study was done to compare more than two groups. Simple linear regression was performed for comparing two continuous variables. P-values of less than 0.05 are considered statistically significant.

CHAPTER 3

RESULTS

3.1. Preparation of CAPP Polymer Films

We began by establishing the optimal conditions for the formation of surface-eroding CAPP films of varying thickness. We determined that CAP:P mixtures dispersed well at 7% w/v in acetone and 70:30 weight ratio CAP:P films evaporated from acetone at 4□C to form uniform and rigid films (Fig. 1A). For drug loading, the active molecules (e.g., rhodamine dye or DOI compound) were co-dissolved in the solution of acetone and became encapsulated in the CAP:P polymer network upon solvent evaporation (Fig. 1B), resulting in highly efficient drug loading into the CAPP films.

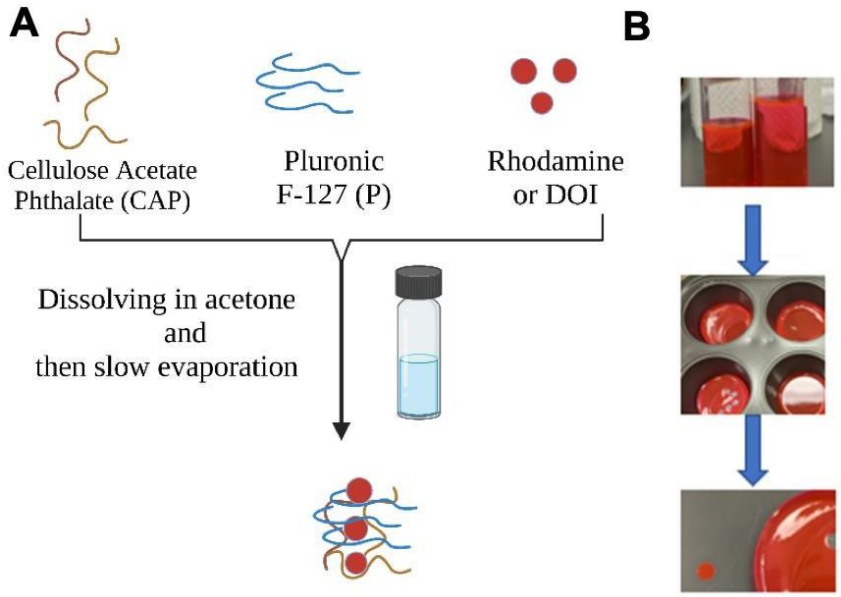

Figure 1. Schematic of CAPP film preparation. (A) Schematic of CAPP film formation by solvent evaporation and drug encapsulation. (B) Representative images of the film production process.

Using Teflon (PTFE)-coated dishes with uniform diameter, we produced films from 300, 600, 900, and 1200 mg of CAPP polymer mixture at the 70:30 CAP:P weight ratio. These reproducibly generated films of ~0.1-, 0.2-, 0.3-, and 0.4-mm thickness, respectively (Fig. 2A), as determined by caliper measurements. Thus, as long as the volume of dishes used for fabrication remained constant, there was a strong linear correlation between polymer mass and thickness of the films, which could be used to accurately produce films of desired thickness for the remainder of the study. To further confirm the thickness and morphology of CAPP films, we cross-sectioned and imaged the films by scanning electron microscopy (SEM). SEM images confirmed the consistent increase in thickness achieved when increasing the polymer mass from 300 – 1200 mg and exhibited that the polymer films form with relatively consistent and smooth surface morphology (Fig. 2B).

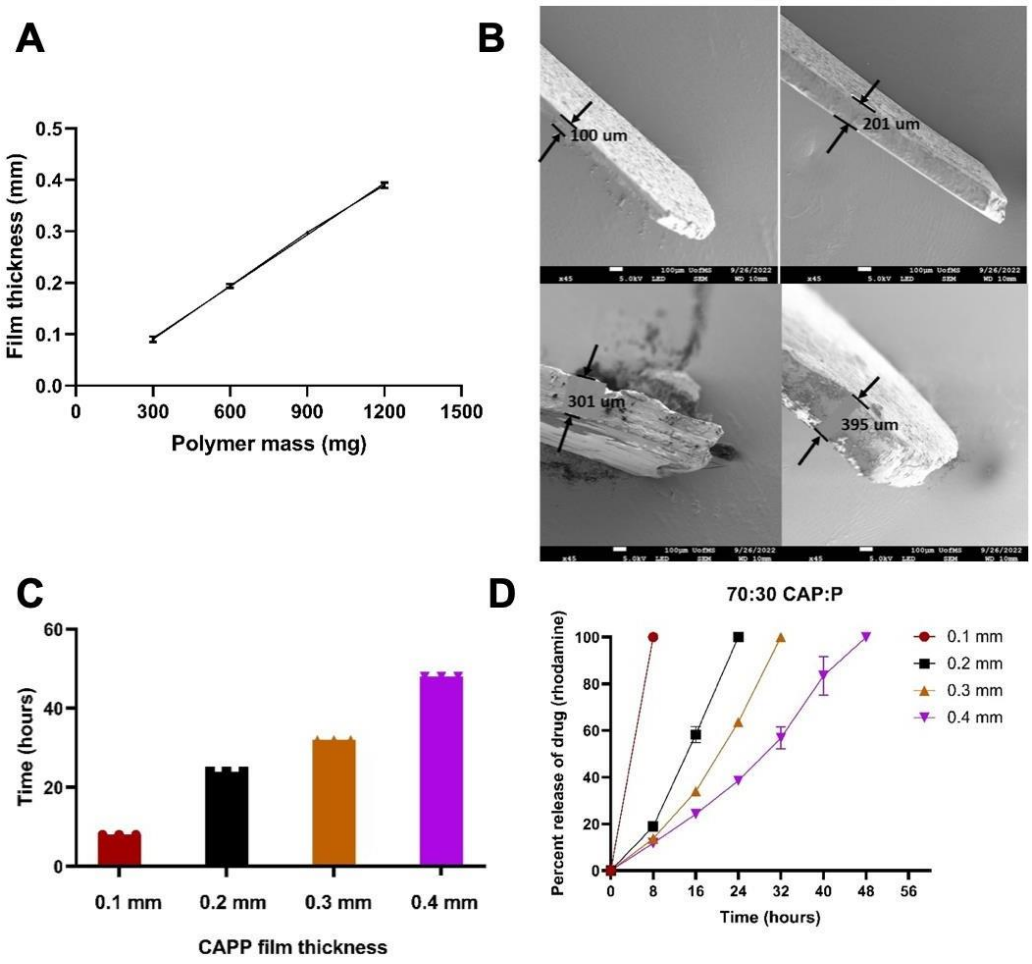

Figure 2. Optimization of the CAPP "release" layer. (A) Film thickness vs. polymer mass. (B) SEM images of cross-sections 0.1-, 0.2-, 0.3-, 0.4 mm films (clockwise) (C) Erosion time vs. film thickness. (D) Cumulative release of Rhodamine from 0.1-0.4 mm films. *Error bars are included for parts A and C, but are not visible due to small error.

3.2. Optimization of the CAPP "Release" Layer

Our next goal – knowing the predictable thicknesses of films based on polymer weight – was to establish any correlation between film thickness and erosion time. To monitor erosion time with the highest degree of accuracy, we monitored the release of rhodamine from

rhodamine-loaded films using a microplate reader. We marked the final erosion time as the time at which rhodamine was no longer detected in releases, indicating that the rhodamine-loaded CAPP films were fully eroded. Additionally, we visually monitored the films to confirm that erosion/degradation of the films had occurred as opposed to just diffusion-based release of the rhodamine from solid/swelled films. We found that erosion time was dependent on the thickness of the films, where 0.1-, 0.2-, 0.3-, and 0.4-mm thick films were fully eroded at 8, 24, 32, and 48 hours, respectively (Fig. 2C). Lastly, we confirmed the highly-tunable controlled release of drug from CAPP films using Rhodamine as a model drug. The CAPP films display a controlled, almost linear release profile over time as they degrade (Fig. 2D). This feature could be used to precisely program the rate and amount of drug release over time from the "release" layer (i.e., the active layer which is loaded with drug) of multilayered CAPP films. Because our goal was to produce rapid pulses of $5HT_{2A}$ agonists for the purpose of microdosing psychedelics, we chose to move forward with 0.1 mm thick CAPP films as the "release" layers.

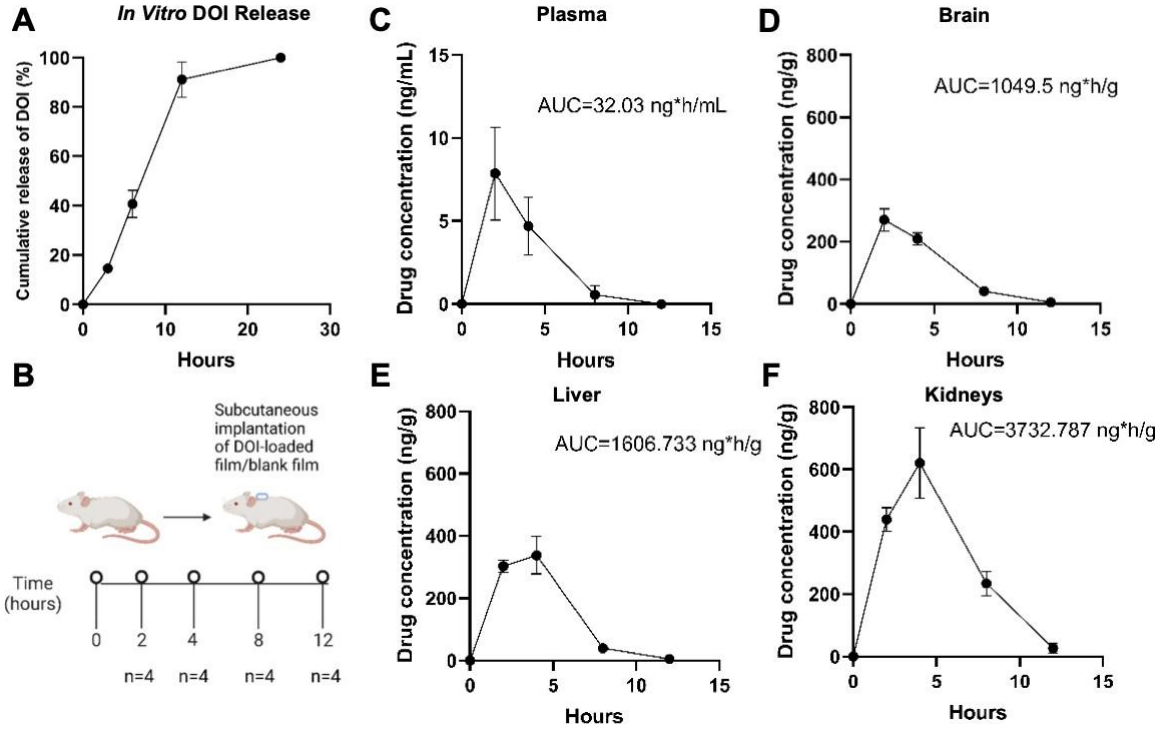

Figure 3. DOI release from single-layered CAPP film *in vitro* and *in vivo*. (A) *In vitro* cumulative release of DOI from 0.1 mm CAPP films. (B) Scheme of subcutaneous implantation and experimental time course. (C-F) Pharmacokinetics and biodistribution of DOI released from subcutaneously implanted, single-layered CAPP films *in vivo*. (n = 4)

3.3. Release of the $5HT_{2A}$ Agonist DOI from CAPP Films

Having determined a feasible design for the "release" layers of multilayered CAPP films, we next confirmed that $5HT_{2A}$ agonists could be loaded and released from CAPP films in a similar manner to rhodamine dye. The $5HT_{2A}$ agonist DOI was loaded into 0.1 mm thick CAPP films, followed by incubation in PBS and collection of releases over time. DOI release proceeded at a very similar rate to the rhodamine dye that was used to optimize the film conditions, and most of the DOI was released by ~8-12 hours incubation in PBS (Fig. 3A). DOI-loaded CAPP films were next implanted subcutaneously on the dorsal region of CD-1 mice, followed by the

pharmacokinetic analysis of DOI 2-, 4-, 8-, and 12-hours post-implantation (Fig. 3B). In agreement with prior literature on DOI and other psychedelics [21], the half-life in the blood plasma was very short, and DOI concentration in the blood returned to undetectable levels by ~8 hours post-implantation (Fig. 3C). Importantly, we detected significant accumulation of DOI in the brain following subcutaneous implantation of the DOI-loaded films, and we observed the maximum concentration (C_{max}) of DOI in the plasma and brain at 2 hours post-implantation (Figs. 3C-D). We also observed a significant accumulation of DOI in major clearance organs such as the liver and kidneys, where the C_{max} was slightly delayed compared to the plasma, occurring at ~4 hours post-implantation (Fig. 3E-F). Cumulatively, these data demonstrate our ability to formulate DOI-loaded CAPP films and achieve systemic absorption and distribution of DOI following subcutaneous implantation of the films.

3.4. Optimization of the CAPP "Blank" Layer.

To produce multilayered CAPP films for pulsed release of DOI *in vivo,* we next had to engineer "blank" CAPP films (i.e., unloaded CAPP films) that could be used as intermediate layers to prevent release during the intermittent, or "off", phases of interval release. Since our goal was to make "blank" layers using the thinnest possible CAPP films, we investigated further the impact of the ratio of CAP:P in the CAPP films on water absorption and erosion time. Based on previous reports [27], we hypothesized that increasing the ratio of CAP would increase the hydrophobicity of the films and significantly retard erosion times. When incubated in PBS, we observed a clear connection between the CAP:P film ratio and the amount of water absorption which was quantified by measuring the change in mass of films before and after incubation in PBS (Fig. 4A). Whereas 70:30 CAPP films increased ~40% in mass after incubation in PBS, 90:10 CAPP films had limited water absorption of ~10% (Fig. 4A). Therefore, we next measured the erosion

time of films at CAP:P ratios of 70:30, 80:20, and 90:10, and did so for the same thicknesses that were investigated previously for the "release" layers (0.1 – 0.4 mm). Again, we observed a clear contribution of the CAP:P ratio, where films with a higher ratio of CAP had significantly extended erosion duration (Fig. 4B). For instance, 90:10 CAPP films had on average 1.52 times longer erosion duration compared to 70:30 CAPP films when averaged across all thicknesses tested. Lastly, we measured rhodamine release over time from both 70:30 and 90:10 CAPP films to gain further insight into the kinetics of film erosion. For all thicknesses tested, 90:10 CAPP films had delayed rhodamine release compared to the 70:30 films (Figs. 4C-F).

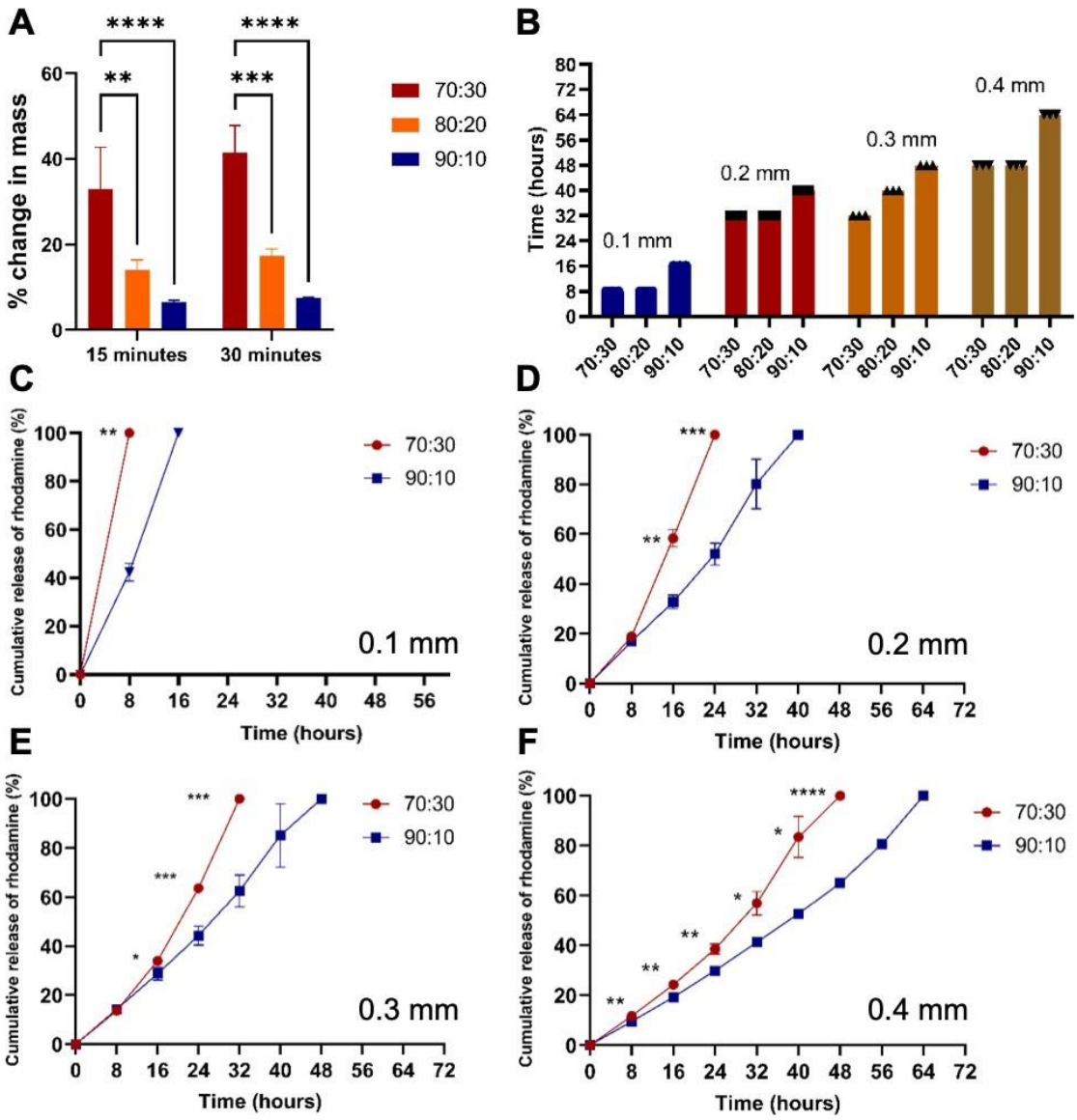

Figure 4. Optimization of the CAPP "Blank" Layer. (A) Water absorption for 70:30-90:10 CAPP films measured by mass of the films before and after incubation in PBS. Two-way ANOVA was performed (n=3). Statistically significant difference is indicated by asterisk, where *p*-value < 0.001 is ***, *p*-value < 0.0001 is ****. (B) Erosion time for 70:30-90:10 CAPP films at each thickness 0.1-0.4 mm. (C-F) Rhodamine release from 70:30 vs 90:10 films at each thickness 0.1-0.4 mm. (n = 3, t-test at each time point, *p*-value < 0.05 is *, *p*-value< 0.01 is **, and *p*-value < 0.001 is ***, *p*-value < 0.0001 is ****).

3.5. Interval Release of Multilayered CAPP Films

We prepared multilayered films based on the scheme in Figure 5A, followed by confirmation of film structure and quantification of drug release from the films. Multilayered films with rhodamine-loaded "release" layers were produced, cross-sectioned, and then imaged using a confocal microscope. Clear and precise loaded layers were visualized, and the layers had consistent thicknesses and spacing between layers (Fig. 5B). After confirmation of film structure, we incubated the multilayered films in PBS at 37 °C and monitored drug release by measuring the fluorescence of rhodamine in supernatants over time. Importantly, we were able to capture three distinct pulses of rhodamine release over time (Fig. 5C), and the peak of each pulse was separated by ~60 hrs.

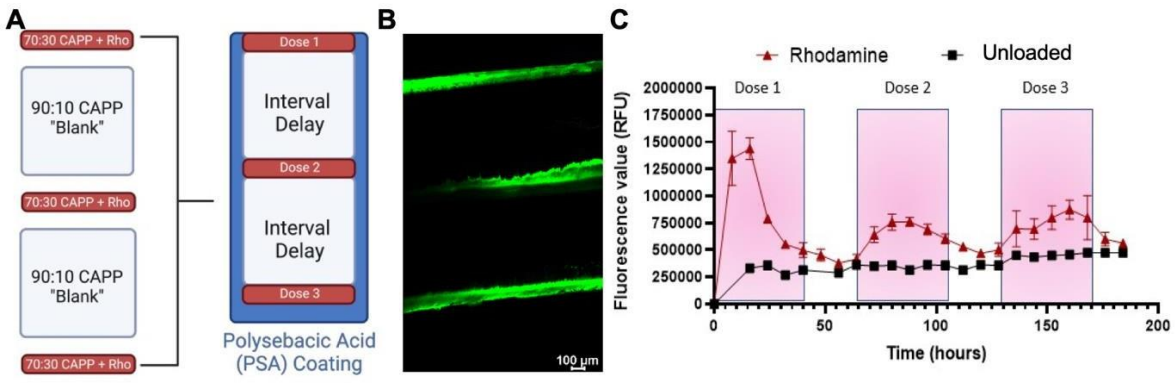

Figure 5. Characterization of Multilayer CAPP films. (A) Schematic representation of multilayer CAPP film design. (B) Representative confocal microscopy image of a multilayered CAPP film cross-section. *Differences in shading are present because it was not possible to get the entire films in a single focal plane. (C) Rhodamine release from Multilayer CAPP films with 3 total doses as indicated in part (A). (n = 3)

3.6. *In Vivo* Interval Delivery of DOI from Multilayered CAPP Films

The final aim of the current study was to show that we could use the multilayered CAPP films to achieve interval drug delivery *in vivo*. To demonstrate pulsed delivery of the $5HT_{2A}$ agonist DOI *in vivo*, we implanted multilayered CAPP films subcutaneously and monitored the pharmacokinetics of DOI post-implantation. The multilayered CAPP films used for this study had the same structure as shown in Figure 5A, but all "release" layers were loaded with 15 μg of DOI (0.75 mg/kg each layer; Fig. S2). The films were then implanted subcutaneously in CD-1 mice, and the pharmacokinetics and biodistribution of DOI were quantified from 2 – 28 hours post-implantation. Within this timeframe, we observed the anticipated pulsed release schedule of DOI with two distinct DOI pulses where peak concentrations in the plasma occurred at ~2 and 20 hours post-implantation (Figure 6A). Moreover, the concentration of DOI in the brain, liver, and kidneys matched the pulsed profile of the blood plasma (Figs. 6B-D).

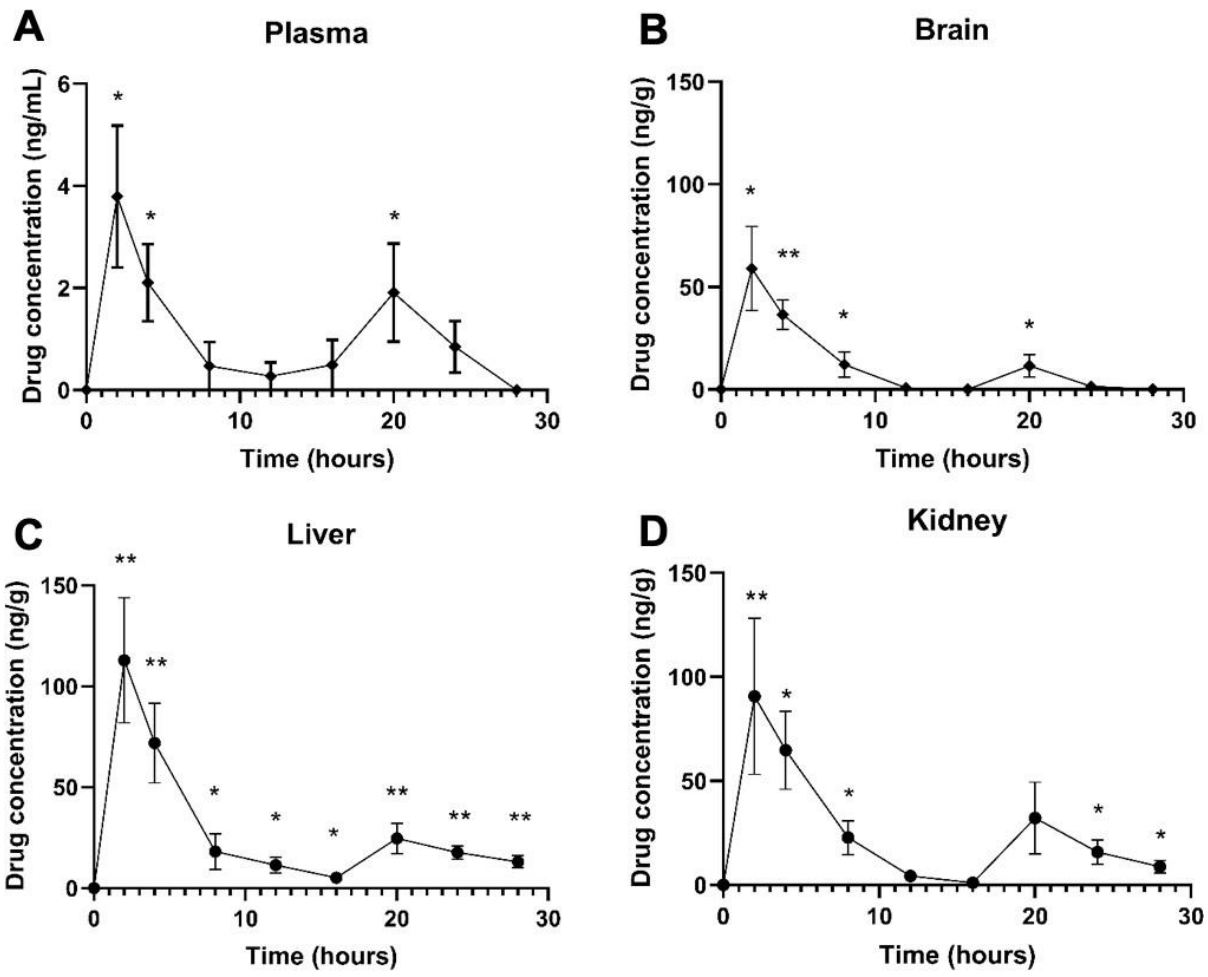

Figure 6. ***In vivo*** **delivery of DOI from multilayer CAPP films**. (A-D) Concentration of DOI in plasma (A), brain (B), liver (C), and kidneys (D) from 2-28 hours post-implantation of multilayered CAPP films. (n = 4). T-test was performed at each time point comparing with unloaded CAPP film implanted mice. Statistically significant difference was observed while comparing each time point of DOI-loaded CAPP film biodistribution data with unloaded CAPP film biodistribution data. The statistical significance is indicated by asterisk, where p-value < 0.05 is *, p-value< 0.01 is **, and p-value less than 0.001 is ***.

As expected, the dissolution of the films was much more rapid *in vivo* than *in vitro*, where pulses occurred ~6x times faster. Although we show only two pulses *in vivo* (to minimize animal

numbers), these proof-of-principle results clearly indicate the intermittent delivery of DOI from subcutaneously implanted CAPP films. In sum, these data highlight our ability to achieve the interval delivery of DOI *in vivo* from the multilayered CAPP films optimized in this study, and importantly, show that DOI is distributed to target (i.e., brain) and clearance organs (i.e., liver and kidneys) upon absorption from the implantation site.

CHAPTER 4

DISCUSSION

Here, we introduced a strategy for the interval delivery of $5HT_{2A}$ agonists from an implantable and fully biodegradable drug delivery system. Interval delivery is achieved by the layering of drug-loaded and unloaded CAPP films in an alternating fashion, followed by unidirectional surface erosion of the multilayered films. We found that the ratio of CAP-to-P in CAPP films and film thickness are both important parameters that can be tuned to modulate the interval release profile. For instance, increasing the CAP content in films was an effective way to exclude water absorption and slow film erosion. Moreover, we observed a direct correlation between film thickness and overall erosion time/drug release kinetics as expected. Finally, we demonstrated that the multilayered CAPP films could deliver distinct pulses of rhodamine (as a model drug) and DOI ($5HT_{2A}$ agonist), and we monitored the pharmacokinetics and biodistribution of DOI upon release from the films in vivo. To our knowledge, this is the first use of a drug delivery system to achieve the interval delivery of $5HT_{2A}$ agonists which make up a large portion of the 'classical psychedelics'.

Having optimized both the drug-loaded "release" and unloaded "blank" CAPP films, we assembled multilayered films and performed proof-of-concept studies to confirm that these films could be used for interval drug release both *in vitro* and *in vivo*. The structure of the multilayered

CAPP films is shown in Figure 5A. The drug-loaded "release" layers are composed of 0.1 mm thick 70:30 CAPP films to ensure rapid dissolution and drug release. The unloaded "blank" layers are composed of two 0.4 mm thick 90:10 CAPP films to separate "release" layers and turn off delivery from the multilayered films for extended periods. Two other design features are worth noting. The bottom of the multilayered films are made up of multiple "blank" layers in order to maintain device structure until the last "release" layer has been fully dissolved. Also, the multilayered CAPP films are coated on all sides but one by a slowly-degrading polymer, poly(sebacic acid) (PSA), to ensure the dissolution of the films proceeds in a single direction. For the current studies, we produced multilayered films with 3 "release" layers separated by 2 "blank" layers as a proof-of-concept that 3 distinct drug pulses could be achieved using these films. However, the films shown here could be layered further to achieve more doses and can be tailored to the need of specific therapeutic applications.

Importantly, 90:10 CAPP films displayed linear, sustained rhodamine release profiles which corroborate prior reports on CAPP films and which are highly suggestive of surface erosion of the films [27], [28],[34], [29]. We also observed that the drug release rate is similar for 70:30 and 90:10 CAPP films at early time points but diverges at later time points, where release from the 70:30 CAPP films seem to accelerate compared to 90:10 CAPP films. This outcome squares well with our observation that water infiltration is much greater in the more hydrophilic 70:30 CAPP films (Fig. 4A). The water infiltration is especially consequential since it is known that hydrogen

bonding is an important driving force of CAPP film formation [35], [27], and water infiltration almost surely disrupts the hydrogen bonding between CAP and P polymers.

Admittedly, we observed wider drug release pulses than originally anticipated. We have noticed that when the films are stacked into multilayered films that both the on- and off-rates of release are much more prolonged as compared to a single film in solution. We hypothesize that there are multiple contributing factors to this phenomenon. In the layered orientation, the films are exposed to water on just one single side, as opposed to being exposed to water from every direction. We find that this consistently results in wider pulses of release as compared to the release kinetics that are achieved with single films. Additionally, we expect that there is some level of diffusion happening within the devices where the drug-loaded layers may slowly spread to surrounding layers. This was one of the motivations for our group to use the 90:10 unloaded blank layers to try and minimize this inter-layer diffusion. However, we cannot rule out the possibility that diffusion is occuring to a certain extent even with the 90:10 unloaded layers.

Others have explored reservoir-based devices to achieve pulsatile release. In these devices, an array of reservoirs is loaded with the drug and each reservoir is sealed with a lid that responds either to electrical activation in the active device [36][15], or is biodegraded at a pre-programmed rate in vivo in the passive device [15]. The active device is 4.5 x 5.5 x 1 cm in volume and requires a minor surgical procedure for implant and explant. Because TRD treatment via microdosing could last years, several surgical procedures would be required, which increases overall treatment cost and increases potential risks to the patient. The passive device is 1.2 cm in diameter and fully biodegradable, but the degradation rate of a reservoir lid is controlled by the molecular weight and/or composition of poly(lactic-co-glycolic acid) (PLGA) in the lid, making it impractical to create the dozens of different polymer compositions required for microdosing over several months.

Fillable microparticles have also been developed for pulsatile release, but would suffer from similar setbacks in this application since using PLGA chemistry to tune the release rate will result in only a few distinct pulses, and therefore, many repeat injections will be needed [37]. Moreover, micropaticles are not recoverable after injection which could cause safety concerns if patients have an adverse reaction to therapy. The films developed here have the advantages of being fully biodegradable so no excision surgery is needed, recoverable if safety concerns arise, and highly programmable to achieve many pulses as well as control over the interval spacing. One shortcoming of the technology could be the reliance on film thickness to control erosion rate which could become impractical for the high number of doses needed per device for the application of microdosing. Therefore, future work will focus on ways to decrease device thickness and tune release by alternative mechanisms such as film chemistry and geometry instead of relying only on CAP:P ratio and film thickness to control release rates.

Although psychedelic drugs, such as the $5HT_{2A}$ agonists LSD, psylocybin, and DOI, show major upside for treating a variety of diseases, their widespread therapeutic use is likely to be hampered by practical barriers, including their designation as Schedule I controlled substances, concerns over abuse/diversion, patient compliance to the complex dosing regimen, and accessibility to therapy. The multilayered CAPP films optimized here are designed to overcome these barriers by providing a fully biodegradable implant capable of interval drug dosing upon implantation. Therefore, concerns over abuse/diversion of the controlled substances would be alleviated due to their embedding in the polymeric films. Additionally, patient compliance is ensured by the delivery of drug at intervals that are automatically pre-programmed by the design of the films, preventing patients from having to visit a clinic for every drug dose.

DOI is a $5HT_{2A}$ agonist in the class of substituted amphetamines that has been reported to reduce depression [38], inflammation [39], and substance abuse [40]. DOI is particularly desirable as a potential anti-depressant because it does not cause any transient anxiety while reducing the symptoms of depression [38]. In the referenced study, DOI reduced behavioral despair/passivity measured by the immobility time in the forced swim test in rodents after a single dose at 2 mg/kg, whereas measures of anxiety, such as locomotor activity in a novel environment and time spent in an illuminated area, showed no induction of anxiety-like behaviors. Instead, structural changes in enhancer chromatin regions linked to anti-depressant characteristics were documented. Additionally, although many psychedelics demonstrate anti-inflammatory properties, DOI more potently reduces pro-inflammatory cytokines compared to others in the drug class [39]. For instance, DOI demonstrated remarkable anti-inflammatory potency in a number of mouse models including direct TNF-α injection [41], allergic asthma [42], and high-fat feeding [43], and these effects are seen at doses below those shown to produce behavioral effects [44]. Thus, DOI was chosen for the current studies not only as a proof-of-principle to demonstrate that interval delivery of $5HT_{2A}$ agonists could be achieved using multilayered CAPP films, but also because DOI delivery from the films could prove to be a powerful therapeutic approach to treat a variety of disorders such as depression and inflammatory disease.

CHAPTER 5

CONCLUSION AND FUTURE DIRECTION

With the granting of "Breakthrough Therapy" status for psilocybin by the FDA in 2018, psychedelics have re-emerged as powerful potential therapeutics for a host of mental health disorders including depression, post-traumatic stress disorder, and addiction. Here, we have demonstrated the ability to encapsulate the psychedelic DOI within multilayered CAPP films and achieve interval release of DOI both in vitro and in vivo. This work serves as proof-of-principle that psychedelics such as DOI can be effectively dosed from implantable drug delivery systems, overcoming a variety of practical barriers to using these compounds as therapeutic agents. Therefore, we anticipate that the DOI-loaded, multilayered CAPP films developed here could significantly aide in the clinical development of psychedelics in medicine and enable unprecedented future studies into the merits of microdosing.

However, this study is still in its preliminary stage. A thorough biocompatibility study with $5HT_{2A}$ agonist-encapsulated multilayered CAPP films need to be done. This proof of study will be clinically compatible if multiple doses of upto 1 year can be loaded in a single polymeric device.

REFERENCES

REFERENCES

[1] A. Kikuchi and T. Okano, "Pulsatile drug release control using hydrogels.," *Adv. Drug Deliv. Rev.*, vol. 54, no. 1, pp. 53–77, Jan. 2002.

[2] J. W. Wheless and S. J. Phelps, "A Clinician's Guide to Oral Extended-Release Drug Delivery Systems in Epilepsy.," *J. Pediatr. Pharmacol. Ther. JPPT Off. J. PPAG*, vol. 23, no. 4, pp. 277–292, 2018.

[3] D. Jain, R. Raturi, V. Jain, P. Bansal, and R. Singh, "Recent technologies in pulsatile drug delivery systems.," *Biomatter*, vol. 1, no. 1, pp. 57–65, 2011.

[4] A. Maroni, L. Zema, M. D. Del Curto, G. Loreti, and A. Gazzaniga, "Oral pulsatile delivery: rationale and chronopharmaceutical formulations.," *Int. J. Pharm.*, vol. 398, no. 1–2, pp. 1–8, Oct. 2010.

[5] L. E. Kalantzi, E. Karavas, E. X. Koutris, and D. N. Bikiaris, "Recent advances in oral pulsatile drug delivery.," *Recent Pat. Drug Deliv. Formul.*, vol. 3, no. 1, pp. 49–63, Jan. 2009.

[6] A. Geraili and K. Mequanint, "Systematic Studies on Surface Erosion of Photocrosslinked Polyanhydride Tablets and Data Correlation with Release Kinetic Models.," *Polymers (Basel).*, vol. 12, no. 5, May 2020.

[7] A. C. Ross, R. J. MacRae, M. Walther, and H. N. Stevens, "Chronopharmaceutical drug delivery from a pulsatile capsule device based on programmable erosion.," *J. Pharm. Pharmacol.*, vol. 52, no. 8, pp. 903–909, Aug. 2000.

[8] K. S. Oh, S. K. Han, Y. W. Choi, J. H. Lee, J. Y. Lee, and S. H. Yuk, "Hydrogen-bonded polymer gel and its application as a temperature-sensitive drug delivery system.," *Biomaterials*, vol. 25, no. 12, pp. 2393–2398, May 2004.

[9] M. J. Webber and D. G. Anderson, "Smart approaches to glucose-responsive drug delivery.," *J. Drug Target.*, vol. 23, no. 7–8, pp. 651–655, 2015.

[10] T. Li *et al.*, "Thermosensitive Hydrogel Co-loaded with Gold Nanoparticles and Doxorubicin for Effective Chemoradiotherapy.," *AAPS J.*, vol. 18, no. 1, pp. 146–155, Jan. 2016.

[11] D. S. Hsieh, R. Langer, and J. Folkman, "Magnetic modulation of release of macromolecules from polymers.," *Proc. Natl. Acad. Sci. U. S. A.*, vol. 78, no. 3, pp. 1863–1867, Mar. 1981.

[12] T. Hoare *et al.*, "Magnetically triggered nanocomposite membranes: a versatile platform for triggered drug release.," *Nano Lett.*, vol. 11, no. 3, pp. 1395–1400, Mar. 2011.

[13] J. Kost, “Ultrasound for controlled delivery of therapeutics.,” *Clin. Mater.*, vol. 13, no. 1–4, pp. 155–161, 1993.

[14] S. A. Stewart, J. Domínguez-Robles, R. F. Donnelly, and E. Larrañeta, “Implantable Polymeric Drug Delivery Devices: Classification, Manufacture, Materials, and Clinical Applications.,” *Polymers (Basel).*, vol. 10, no. 12, Dec. 2018.

[15] J. H. Prescott *et al.*, “Chronic, programmed polypeptide delivery from an implanted, multireservoir microchip device.,” *Nat. Biotechnol.*, vol. 24, no. 4, pp. 437–438, Apr. 2006.

[16] J. H. Prescott, T. J. Krieger, S. Lipka, and M. A. Staples, “Dosage form development, in vitro release kinetics, and in vitro-in vivo correlation for leuprolide released from an implantable multi-reservoir array.,” *Pharm. Res.*, vol. 24, no. 7, pp. 1252–1261, Jul. 2007.

[17] P. E. Greenberg *et al.*, “The Economic Burden of Adults with Major Depressive Disorder in the United States (2010 and 2018).,” *Pharmacoeconomics*, vol. 39, no. 6, pp. 653–665, Jun. 2021.

[18] D. Amital, L. Fostick, A. Silberman, M. Beckman, and B. Spivak, “Serious life events among resistant and non-resistant MDD patients.,” *J. Affect. Disord.*, vol. 110, no. 3, pp. 260–264, Oct. 2008.

[19] R. G. Dos Santos, J. E. Hallak, G. Baker, and S. Dursun, “Hallucinogenic/psychedelic $5HT_{2A}$ receptor agonists as rapid antidepressant therapeutics: Evidence and mechanisms of action.,” *J. Psychopharmacol.*, vol. 35, no. 4, pp. 453–458, Apr. 2021.

[20] R. L. Carhart-Harris *et al.*, “Psilocybin with psychological support for treatment-resistant depression: an open-label feasibility study.,” *The lancet. Psychiatry*, vol. 3, no. 7, pp. 619–627, Jul. 2016.

[21] R. L. Carhart-Harris *et al.*, “Psilocybin with psychological support for treatment-resistant depression: six-month follow-up.,” *Psychopharmacology (Berl).*, vol. 235, no. 2, pp. 399–408, Feb. 2018.

[22] R. L. Carhart-Harris and D. J. Nutt, “Serotonin and brain function: a tale of two receptors.,” *J. Psychopharmacol.*, vol. 31, no. 9, pp. 1091–1120, Sep. 2017.

[23] R. L. Carhart-Harris and G. M. Goodwin, “The Therapeutic Potential of Psychedelic Drugs: Past, Present, and Future.,” *Neuropsychopharmacol. Off. Publ. Am. Coll. Neuropsychopharmacol.*, vol. 42, no. 11, pp. 2105–2113, Oct. 2017.

[24] R. E. Daws *et al.*, “Increased global integration in the brain after psilocybin therapy for depression.,” *Nat. Med.*, vol. 28, no. 4, pp. 844–851, Apr. 2022.

[25] B. V. Burdick and B. Adinoff, “A proposal to evaluate mechanistic efficacy of hallucinogens in addiction treatment.,” *Am. J. Drug Alcohol Abuse*, vol. 39, no. 5, pp. 291–297, Sep. 2013.

[26] A. K. Bershad, S. T. Schepers, M. P. Bremmer, R. Lee, and H. de Wit, “Acute Subjective and Behavioral Effects of Microdoses of Lysergic Acid Diethylamide in Healthy Human Volunteers.,” *Biol. Psychiatry*, vol. 86, no. 10, pp. 792–800, Nov. 2019.

[27] A. T. Raiche and D. A. Puleo, “Association polymers for modulated release of bioactive proteins.,” *IEEE Eng. Med. Biol. Mag. Q. Mag. Eng. Med. Biol. Soc.*, vol. 22, no. 5, pp. 35–41, 2003.

[28] J. H. Jeon, M. V Thomas, and D. A. Puleo, “Bioerodible devices for intermittent release of simvastatin acid.,” *Int. J. Pharm.*, vol. 340, no. 1–2, pp. 6–12, Aug. 2007.

[29] J. H. Jeon and D. A. Puleo, “Alternating release of different bioactive molecules from a complexation polymer system.,” *Biomaterials*, vol. 29, no. 26, pp. 3591–3598, Sep. 2008.

[30] J. H. Jeon and D. A. Puleo, “Formulations for intermittent release of parathyroid hormone (1-34) and local enhancement of osteoblast activities.,” *Pharm. Dev. Technol.*, vol. 13, no. 6, pp. 505–512, 2008.

[31] S. C. Sundararaj, M. V Thomas, T. D. Dziubla, and D. A. Puleo, “Bioerodible system for sequential release of multiple drugs.,” *Acta Biomater.*, vol. 10, no. 1, pp. 115–125, Jan. 2014.

[32] S. C. Sundararaj, M. Al-Sabbagh, C. L. Rabek, T. D. Dziubla, M. V Thomas, and D. A. Puleo, “Comparison of sequential drug release in vitro and in vivo.,” *J. Biomed. Mater. Res. B. Appl. Biomater.*, vol. 104, no. 7, pp. 1302–1310, Oct. 2016.

[33] N. Venkatesan *et al.*, “Biodegradable polymerized simvastatin stimulates bone formation.,” *Acta Biomater.*, vol. 93, pp. 192–199, Jul. 2019.

[34] J. H. Jeon, W. T. Piepgrass, Y.-L. Lin, M. V Thomas, and D. A. Puleo, “Localized intermittent delivery of simvastatin hydroxyacid stimulates bone formation in rats.,” *J. Periodontol.*, vol. 79, no. 8, pp. 1457–1464, Aug. 2008.

[35] X. Xu and P. I. Lee, “Programmable drug delivery from an erodible association polymer system.,” *Pharm. Res.*, vol. 10, no. 8, pp. 1144–1152, Aug. 1993.

[36] R. Farra *et al.*, “First-in-human testing of a wirelessly controlled drug delivery microchip.,” *Sci. Transl. Med.*, vol. 4, no. 122, p. 122ra21, Feb. 2012.

[37] K. J. McHugh *et al.*, “Fabrication of fillable microparticles and other complex 3D microstructures.,” *Science*, vol. 357, no. 6356, pp. 1138–1142, Sep. 2017.

[38] M. de la Fuente Revenga *et al.*, “Prolonged epigenomic and synaptic plasticity alterations following single exposure to a psychedelic in mice.,” *Cell Rep.*, vol. 37, no. 3, p. 109836, Oct. 2021.

[39] T. W. Flanagan and C. D. Nichols, “Psychedelics as anti-inflammatory agents.,” *Int. Rev. Psychiatry*, vol. 30, no. 4, pp. 363–375, Aug. 2018.

[40] A. Oppong-Damoah, K. E. Curry, B. E. Blough, K. C. Rice, and K. S. Murnane, “Effects of the synthetic psychedelic 2,5-dimethoxy-4-iodoamphetamine (DOI) on ethanol consumption and place conditioning in male mice.,” *Psychopharmacology (Berl).*, vol. 236, no. 12, pp. 3567–3578, Dec. 2019.

[41] F. J. Nau, B. Yu, D. Martin, and C. D. Nichols, “Serotonin 5-HT2A receptor activation blocks TNF-α mediated inflammation in vivo.,” *PLoS One*, vol. 8, no. 10, p. e75426,

2013.

[42] F. J. Nau *et al.*, "Serotonin 5-HT_2 receptor activation prevents allergic asthma in a mouse model.," *Am. J. Physiol. Lung Cell. Mol. Physiol.*, vol. 308, no. 2, pp. L191-8, Jan. 2015.

[43] T. W. Flanagan, M. N. Sebastian, D. M. Battaglia, T. P. Foster, E. L. Maillet, and C. D. Nichols, "Activation of 5-HT(2) Receptors Reduces Inflammation in Vascular Tissue and Cholesterol Levels in High-Fat Diet-Fed Apolipoprotein E Knockout Mice.," *Sci. Rep.*, vol. 9, no. 1, p. 13444, Sep. 2019.

[44] R. L. Smith, R. J. Barrett, and E. Sanders-Bush, "Discriminative stimulus properties of 1-(2,5-dimethoxy-4-iodophenyl)-2-aminopropane [(+/-)DOI] in C57BL/6J mice.," *Psychopharmacology (Berl).*, vol. 166, no. 1, pp. 61–68, Feb. 2003.

APPENDIX

Table 1: Erosion Time vs. Film Thickness												
	0.1 mm film			0.2 mm film			0.3 mm film			0.4 mm film		
Time to fully erode films (hours)	8	8	8	24	24	24	32	32	32	48	48	48

Table 2: Cumulative release of Rhodamine from 0.1-0.4 mm films.												
Time (hours)	Cumulative release of rhodamine (%) from 0.1 mm film			Cumulative release of rhodamine (%) from 0.2 mm film			Cumulative release of rhodamine (%) from 0.3 mm film			Cumulative release of rhodamine (%) from 0.4 mm film		
0	0	0	0	0	0	0	0	0	0	0	0	0
8	100	100	100	19.79	17.87	18.89	12.041	14.646	14.375	11.10	11.35	12.76
16				64.94	56.76	53.17	32.987	33.857	35.088	24.09	22.46	26.03
24				100	100	100	64.56	63.49	62.73	36.93	36.02	42.65
32							100	100	100	52.24	51.98	66.40
40										73.89	76.51	100
48										99.99	99.99	

Table 3: *In vitro* cumulative release of DOI from 0.1 mm CAPP films.

Time (hours)	Plasma DOI (ng/mL)			
0	0	0	0	0
2	12.60	7.82	11	0
4	7.49	4.06	7.2	0
8	2.26	0	0	0
12	0	0	0	0

Table 4: Concentration of DOI in mouse plasma at different time points after implantation of a single DOI-loaded 0.1 mm film

Time (hours)	DOI hydrochloride		
0	0	0	0
3	15.72	16.14	12.08
6	43.55	48.45	30.05
12	98.43	98.16	76.76
24	100	100	100

Table 5: Concentration of DOI in mouse brain at different time points after implantation of single DOI-loaded 0.1 mm film

Time (hours)	Brain DOI (ng/g)			
0	0	0	0	0
2	339	224	246	-
4	225	171	231	-
8	28.1	30.02	47.5	58.10
12	10.80	0	0	10.90

Table 6: Concentration of DOI in mouse liver at different time points after implantation of single DOI-loaded 0.1 mm film

Time (hours)	Liver DOI (ng/g)			
0	0	0	0	0
2	299	271	339	-
4	450	245	318	-
8	28.8	27.8	41.3	59.4
12	10.40	0	0	8.4

Table 7: Concentration of DOI in mouse kidney at different time points after implantation of a single DOI-loaded 0.1 mm film

Time (hours)	Kidney DOI (ng/g)			
0	0	0	0	0
2	400	402	515	-
4	405	667	790	-
8	275	157	269	143
12	74.3	5.96	6.92	20.20

Table 8: Water absorption for 70:30-90:10 CAPP films measured by mass of the films before and after incubation in PBS

	70:30 CAP:P Weight Change (%)			80:20 CAP:P Weight Change (%)			90:10 CAP:P Weight Change (%)		
15 minutes	43.81	30.17	24.78	15.38	11.65	15.55	6.77	6.15	6.83
30 minutes	48.57	39.66	36.28	18.68	15.53	17.78	7.52	7.69	7.56

Table 9: Erosion time for 70:30-90:10 CAPP films at each thickness 0.1-0.4 mm.

CAP:P film	Erosion time (hours) for 0.1 mm film			Erosion time (hours) for 0.2 mm film			Erosion time (hours) for 0.3 mm film			Erosion time (hours) for 0.4 mm film		
70:30	8	8	8	24	24	24	32	32	32	48	48	48
80:20	8	8	8	32	32	32	40	40	40	48	48	48
90:10	16	16	16	40	40	40	48	48	48	64	64	64

Table 10: Concentration of DOI in mouse plasma at different time points after implantation of multilayered DOI-loaded film

Time (hours)	Plasma DOI (ng/mL)			
0	0	0	0	0
2	6.7	4.3	0	4.17
4	2.81	0	2.1	3.49
8	0	1.89	0	0
12	1.09	0	0	0
16	1.96	0	0	0
20	4.67	1.79	1.26	0
24	2.01	1.37	0	0
28	0	0	0	0

Table 11: Concentration of DOI in mouse brain at different time points after implantation of multilayered DOI-loaded film

Time (hours)	Brain DOI (ng/g)			
0	0	0	0	0
2	111.00	71.60	18.90	34.40
4	53.30	22.30	26.50	44.10
8	29.40	8.69	10.50	0
12	0	0	3.30	0
16	0	0	0	0
20	27.70	4.18	7.41	6.73
24	0	6.11	0	0
28	0	0	0	0

Table 12: Concentration of DOI in mouse liver at different time points after implantation of multilayered DOI-loaded film

Time (hours)	Liver DOI (ng/g)			
0	0	0	0	0
2	161.00	146.00	23.10	121.70
4	109.8	27.50	49.90	100.40
8	39.90	7.99	24.80	0
12	3.30	16.30	20.00	5.96
16	6.13	8.94	0	5.46
20	45.40	15.50	26.20	11.8
24	26.10	17.40	18.00	9.05
28	18.7	4.5	12.40	16.40

Table 13: Concentration of DOI in mouse Kidney at different time points after implantation of multilayered DOI-loaded film

Time (hours)	Kidney DOI (ng/g)			
0	0	0	0	0
2	199.00	43.50	36.60	83.50
4	72.70	25.60	47.40	113.30
8	45.30	7.68	22.90	15.30
12	0	7.21	9.80	0
16	0	4.09	0	0
20	83.70	11.70	21.20	11.9
24	13.7	12.9	32.1	4.5
28	11.5	0	10.00	13.70

VITA

Mehjabeen Hossain is from Cox's Bazar, Bangladesh. She received her bachelor's in Genetic Engineering & Biotechnology from the University of Chittagong, Bangladesh in 2012 and a Master's in Infection & Immunity from the Erasmus University medical Center, the Netherlands in 2018. She started her graduate study in Pharmaceutical Sciences (emphasis on Pharmacology) in Fall'2019 at the University of Mississippi under the supervision of Dr. Thomas A Werfel. She worked on the design and production of drug delivery device to deliver $5HT_{2A}$ agonists.